




Cite this: DOI: 10.1039/d6fo00231e

Peptidomic profiling of *in vitro* digesta from diverse microalgae species

Sara Hamzelou,^a  ^{*}a Damien Belobrajdic,^{a,b,c} Henri Brook,^a Wei Chen,^d Fletcher Hiten,^a Kim Lee Chang,^e Diane Purcell,^f Utpal Bose,^d Simone Osborne,^d Cassandra Pegg^d and Michelle L. Colgrave^{*d,g}

Microalgae are a sustainable protein source, yet few species are used for human nutrition. This study evaluated eight species for protein quality, digestibility, and peptide profiles after simulated gastrointestinal digestion using INFOGEST. Amino acid content, and intestinal-phase peptide mixtures were analysed by mass spectrometry. The methanol precipitation method was used to separate digested (supernatant) and undigested (pellet) peptides following *in vitro* INFOGEST digestion. The pellet was further separated by molecular weight into 3–10 kDa and >10 kDa fractions to isolate the lower molecular weight peptides from the higher ones. This separation method enabled the identification of potential digested peptides within the 3–10 kDa fraction that may still be present in the pellet. Cell-based and *in silico* analysis showed the 3–10 kDa fraction contained permeable peptides, highlighting 80% methanol's limitation in recovering all digestible peptides in the INFOGEST protocol. However, discrepancies between *in silico* predictions and *in vitro* permeability revealed that machine learning approaches alone are insufficient, underscoring the critical importance of experimental validation. The >10 kDa fraction predominantly contained structural proteins for photosynthesis, indicating digestion resistance. *Pandorina* sp. and *Glaucozystis nostochinearum* exhibited essential amino acid-rich profiles, especially their high Lysine content which is a limiting amino acid in most plant-derived proteins. These findings reveal digested microalgae's peptide composition and potential as functional food ingredients.

Received 16th January 2026,

Accepted 30th April 2026

DOI: 10.1039/d6fo00231e

rsc.li/food-function

1. Introduction

Microalgae are a diverse group of microorganisms known for their nutritional richness, offering proteins, dietary fibre, polyunsaturated fatty acids, antioxidants, and bioactive compounds. Certain microalgae species accumulate significant amounts of protein in their biomass, positioning them as a promising complementary protein source for human diets.^{1,2} Additionally, microalgae production offers substantial environmental advantages over traditional animal and plant-based diets, including high biomass and protein yields, rapid growth rates, and the capacity to be cultivated on non-arable land.³ However, the

nutritional profile and digestive profiles have yet to be established to use them as a complementary protein source.

While numerous studies have focused on maximising protein extraction from microalgae to increase yield,¹ less attention has been given to assessing the quality and nutritional value of these proteins. Protein quality is primarily determined by the profile of essential amino acids (EAA) and their ileal digestibility, factors that directly influence the nutritional value of microalgae. Advances in mass spectrometry, particularly in the emerging field of digestomics, now enable the detailed identification and quantification of peptide digests and amino acids generated during protein digestion.⁴

Nutrient absorption—including that of proteins, carbohydrates, lipids, and minerals—occurs primarily in the small intestine, which plays a central role in human digestion.⁵ While the most accurate assessment of protein digestibility is obtained through ileal measurements in humans, this approach is often limited by practical and ethical constraints. Animal models, like ileum-fistulated pigs and rats, are frequently used but are expensive and present ethical considerations. As an alternative, *in vitro* digestion protocols provide a reproducible, validated, and non-invasive method for simulating human digestive processes, which is particularly valuable

^aCSIRO Health & Biosecurity, Adelaide, SA, 5000, Australia^bAlliance for Research in Exercise, Nutrition and Activity (ARENA), University of South Australia, Adelaide, SA 5001, Australia^cMedicine and Public Health, Health Flinders University, Adelaide, SA 5042, Australia^dCSIRO Agriculture and Food, St Lucia, QLD, 4036, Australia^eCSIRO Environment, Hobart, Tasmania, 7004, Australia^fCSIRO NCMI, Hobart, Tasmania, 7004, Australia^gAustralian Research Council Centre of Excellence for Innovations in Peptide and Protein Science, School of Science, Edith Cowan University, Joondalup, WA, 6027, Australia

when evaluating novel food sources.^{6,7} This aligns with FAO/WHO recommendations to develop *in vitro* methods that accurately predict protein digestibility and bioavailability in humans.⁸ The static *in vitro* digestion model, developed by the European Cooperation in Science and Technology (COST) Action INFOGEST in 2014, closely mimics human physiology and is now widely accepted as a method for studying protein digestibility in food.^{6,9}

The current research on microalgae proteins emphasizes the characterisation of permeable peptides and the quantification of free amino acids, aiming to identify health-promoting bioactive peptides and EAAs beneficial for human nutrition. However, profiling the peptides that remain undigested after simulated digestion is also valuable, as it can reveal structural protein domains that are resistant to gastrointestinal digestion. Thus, analysis of bioactive peptides after the small intestinal digestion process is important, as it provides an indication of those peptides that have the potential to be absorbed in the small intestine or pass into the large intestine, where they can influence the microbiome.^{10,11}

In the present study, we investigated the protein digestibility and peptide profiles—digested and undigested—of eight different species of microalgae. These include green species (*Chlamydomonas* sp., *Desmodesmus arthrodesmiformis*, *Pandorina* sp., *Nannochloropsis australis*) to blue-green consisting of *Snowella* sp., *Glaucozystis Nostochinearum*, *Arthrospira platensis*) and a red species (*Rhodomonas salina*).

While some microalgae are already approved for human consumption, the incorporation of new species or derived products (e.g., protein isolates) into food systems may require comprehensive regulatory evaluation, such as under the European Union “Novel Food” framework.¹² Among the species investigated in this study, *Arthrospira platensis* is well established for human consumption and is classified as Generally Recognised As Safe (GRAS), having been approved by the United States Food and Drug Administration (FDA) as a dietary supplement since 2003.^{12,13} *Nannochloropsis* sp. has attracted increasing attention due to their high nutritional value, particularly as sources of essential fatty acids and bioactive peptides.¹⁴ Similarly, *Rhodomonas salina* is widely utilised in aquaculture as a high-value live feed due to its favour-

able lipid composition and phycoerythrin content,¹⁵ and is emerging as a promising candidate for human food applications, particularly for its nutritional and colour-enhancing properties. *Pandorina* sp., *Glaucozystis nostochinearum*, *Desmodesmus arthrodesmiformis*, *Chlamydomonas* sp., and *Snowella* sp. are not currently established as food sources. However, these species were selected for this study due to their biochemical diversity and potential as novel sources of functional compounds. All strains were obtained from a controlled culture collection, ensuring consistency and suitability for exploratory biochemical and digestion studies.

In vitro digestion assays were conducted on freeze-dried, disrupted algal cells, followed by mass spectrometric identification of the peptides generated during intestinal digestion. To our knowledge, this is the first study to comprehensively map the peptidome (digestome) of digested microalgal samples.

2. Materials and methods

Microalgae cultivation and sample collection

Eight microalgal species were obtained from the Australian National Algae Culture Collection (ANACC) (Table 1). Each 10 L batch was inoculated with 100 mL of starter culture in Nalgene™ 10 L polypropylene carboys with three biological replicates per species, and incubated for at least 14 days until the cells reached the late exponential growth phase. Cultivation was conducted in controlled environment rooms under cool white, fluorescent light (80–100 μmol photons per m² per s PAR) with a 12 : 12 h light/dark cycle. The incubation temperatures were set at 15 °C, 20 °C, or 25 °C (Table 1), depending on each strain's natural environment.

Biomass was harvested by centrifugation at 3400g for 20 min at 20 °C. The resulting supernatant was discarded, and the pellet was resuspended and washed with sterile 3.15% (w/v) ammonium formate solution and freeze-dried for analysis.

Sample preparation and *in vitro* digestion (IVD)

The nitrogen content of freeze-dried microalgal biomass was measured using the Dumas combustion method on an

Table 1 Taxonomic and culture details of microalgal species used in the study

Row	Taxonomic class	ANACC identifier	Microalgae species	Growth temperature	Source	Culture media
1	Cyanophyceae	CS-697	<i>Arthrospira platensis</i>	25	Taiwan	1/2 MLA ^a -1/2 F/2 ^b
2	Chlorophyceae	CS-977	<i>Chlamydomonas</i> sp.	20	Australia (Tasmania)	MLA freshwater
3	Chlorophyceae	CS-950	<i>Desmodesmus arthrodesmiformis</i>	20	Australia (Victoria)	MLA freshwater
4	Glaucophyceae	CS-777	<i>Glaucozystis Nostochinearum</i>	20	Australia (Western Australia)	MLA ground pool water
5	Eustigmatophyceae	CS-416	<i>Nannochloropsis australis</i>	20	Australia (Tasmania)	F2 Marine
6	Chlorophyceae	CS-946	<i>Pandorina</i> sp.	15	Australia (Victoria)	MLA freshwater
7	Cryptophyceae	CS-174	<i>Rhodomonas salina</i>	20	USA (Connecticut)	GSe marine ^c
8	Cryptophyceae	CS-1224	<i>Snowella</i> sp.	15	Australia (Tasmania)	MLA freshwater

^a Modified liquid medium.¹⁶ ^b Guillard's f/2 marine microalgal growth medium.¹⁷ ^c GSe medium, a variation of G with the addition of 1 × 10⁻⁸ mol L⁻¹ selenium.¹⁸



Elementar CHNS analyser (Langensfeld, Germany), with a nitrogen conversion factor of 4.78 which is widely recommended for microalgae.¹⁹ Cell wall disruption was performed by using ball-milling method. Samples were first ground to a fine powder using a Retsch MM200 mixer mill (Retsch, Inc., Newtown, PA) for 5 min.

Portions equivalent to 40 mg of protein were subjected to the *in vitro* gastrointestinal INFOGEST method.²⁰ The enzyme activities and bile concentrations were determined according to the standardized protocol described by Minekus *et al.*, 2014 *in vitro*.²⁰

In brief, the samples were dissolved in 1 mL of water, and mixed with 1 mL of simulated salivary fluid (pH 7, 37 °C, 300 U mL⁻¹ amylase) for 2 min, then combined with 2 mL of simulated gastric fluid (pH 3, containing 2000 U mL⁻¹ pepsin) and incubated for 120 min at 37 °C. Afterwards, 4 mL of simulated intestinal juice (pH 7) containing pancreatin (100 U trypsin activity per mL) and bile (10 mmol L⁻¹) were added and incubated for 120 min at 37 °C with constant gentle mixing.

Sample separation into digested and undigested fractions was performed using the method described by⁷ with minor modifications.

Peptide samples were separated into digested and undigested fractions by precipitation with methanol to a final concentration of 80% (v/v) at -20 °C for 1 h, followed by centrifugation at 2000g for 10 min at 4 °C. The supernatants were collected, and the pellets were washed using 80% (v/v) methanol, with repeated centrifugation between washes. Both pellets and supernatant (considered as undigestible and digested fraction respectively) were dried and stored at -20 °C for further analysis.

Amino acid analysis

Amino acid profiles (excluding tryptophan and cysteine) were determined for both pellet and supernatant fractions by acid hydrolysis, followed by liquid chromatography-mass spectrometry (LC-MS) as described previously in Hamzelou, Belobrajdic.¹

Sample preparation for LC-MS/MS analysis

Both supernatant and pellet fractions from INFOGEST were dried in a Savant SpeedVac SPD140DDA vacuum concentrator (Thermo Fisher, Waltham, MA, USA).

Supernatants were resuspended in 500 µL of 25% (v/v) acetonitrile containing 1% (v/v) formic acid, filtered (0.2 µm nylon) and transferred to vials for LC-MS/MS analysis.

Pellet fractions were resuspended in 8 M urea, 100 mM Tris-HCl (pH 8.8) and processed to obtain two size fractions: 3–10 kDa and >10 kDa. To obtain the 3–10 kDa fraction, first urea was removed from the samples using Amicon® Ultra Centrifugal Filter, 3 kDa MWCO (Merck Millipore, Bayswater, Vic, Australia) by inverting the filter units and spinning down samples into recovery tube at 1000g for 2 min. The concentrated samples were then loaded on Amicon® Ultra Centrifugal Filter, 10 kDa MWCO (Merck Millipore, Bayswater, Vic, Australia) and the flow through were collected. Peptide

samples then desalted using Pierce™ peptide desalting spin columns (Pierce Biotechnology, Rockford, IL, USA). The >10 kDa fractions were obtained by using filter-aided sample preparation (FASP)¹⁴ by transferring the resuspended pellet in urea to 10 kDa MWCO filters (Merck Millipore, Bayswater, Vic, Australia). All peptide concentrations were determined by micro-BCA assay (Pierce Biotechnology, Rockford, IL, USA) according to the manufacturer's instructions and expressed as mg mL⁻¹. Measurements were performed in triplicate for each sample across three independent biological replicates.

LC-MS/MS analysis of peptide fractions

Peptide profiling of supernatant fractions was conducted on LCMS-9030 mass spectrometer (Shimadzu, Kyoto, Japan) coupled to a Nexera-x3 Ultra Performance Liquid Chromatography (UPLC) system (Shimadzu). Peptides (10 µL) were separated on a Kinetex F5 column (2.1 × 100 mm, 2.6 µm; Phenomenex, Torrance, CA, USA). Peptides were eluted from the column over 30 min, starting with 100% buffer A (0.1% (v/v) formic acid) and holding for 5 minutes, then using a linear solvent gradient with steps from 0 to 30% of buffer B (99.9% (v/v) ACN, 0.1% (v/v) formic acid) for 20 min and 30 to 80% (v/v) of buffer B for 5 min. The mass spectrometer was operated in positive ion mode, measuring full MS1 mass spectra from *m/z* 70 to 1000 throughout the run. MS/MS analysis was conducted on the 20 most intense ions measured between *m/z* 240 and 1000, with a cycle time of 100 ms per precursor. Fragmentation was induced by collision energy ramp from 13 to 47 normalised collision energy units. The source voltage was 2.0 kV, with a nebulising gas flow of 3.0 L min⁻¹, heater gas flow of 10 L min⁻¹, interface temperature of 300 °C, drying gas flow of 10 L min⁻¹, desolvation line temperature of 250 °C, and heater block temperature of 400 °C. Argon was used for the collision gas and nitrogen for the drying gas.

The 3–10 kDa and >10 kDa fractions (0.25 µg peptide) were analysed using a ZenoTOF 7600 mass spectrometer (SCIEX Redwood City, CA, USA) coupled to an ACQUITY UPLC M-Class system (Waters, Massachusetts, USA). Peptides were separated on a C18 column (300 µm × 150 mm, 1.8 µm, 100 Å, Waters) at 40 °C at a flow rate of 5 µL min⁻¹. Peptides were eluted using a 30 min gradient with the same buffers described above, starting with 3% to 35% buffer B for 20 min followed 35–80% buffer B for 2 min and then holding for 1 min at 80% buffer B. The column was then equilibrated with 3% buffer B for 5 min. The source parameters were set at follows: spray voltage at 5000 V; curtain gas at 35; collisional activated dissociation (CAD) gas at 7; and ion source gases 1 and 2 at 20 psi and 15 psi, respectively. TOF MS scans were acquired across a mass range of *m/z* 350–1750; with accumulation time of 0.2 seconds, a decluttering potential of 80 V, and a collision energy of 10 V. The top 20 precursors were selected for MS2 with charge states between 1–4 and excluding precursors for 5 s after two occurrences. Parameters included a mass range of *m/z* 100–1500; dynamic collision-induced dissociation (CID), Zeno pulsing enabled, an accumulation time of 0.025 seconds, and summation of 8-time bins.



Peptide identification and mass spectrometry data processing

A custom reference database (737 532 protein sequences) was compiled from UniProt KB and NCBI entries from all microalgal species (September 2024). The database included *Arthrospira platensis* (13 102 protein sequences), *Chlamydomonas* sp. (116 001 protein sequences), *Snowella* sp. (4285 protein sequences), *Nannochloropsis* sp. (25 580 protein sequences), *Glaucocystis* sp., (420 protein sequences), and *Chlorophyceae* (331 001 after removing the sequence duplicates) downloaded from UniProt KB. The database also included *Rhodomonas* sp. (79 984 protein sequences) and translated *Desmodesmus* reference genome (210 998 protein sequences) downloaded from NCBI. The later was created from the contigs derived from the *Desmodesmus* reference genome assembly ASM744998v2 to predict open reading frames (ORFs) with a minimum cut-off of 100 bp using CLC Main Workbench version 24.0.2.

Mass spectrometry data processing and peptide identification for all three fractions were performed *via* Peaks Studio version 11.0 software (Bioinformatics Solutions, Waterloo, ON, Canada) using our custom database for >10 kDa fraction. Searches were performed with nonspecific (no-enzyme) digestion, a precursor mass tolerance of 20 ppm, and a fragment ion tolerance of 0.2 Da. Cysteine carbamidomethylation was set as fixed modification for >10 kDa fraction and methionine oxidation and deamidation were chosen as variable modifications. Only *de novo* sequenced peptides with an average local confidence (ALC) score of $\geq 80\%$ were retained. *De novo* sequence tags were used by PEAKS DB to be searched against our database. False discovery rate (FDR) analysis was set to 1% for peptide-spectrum matches (PSMs).

Cell culture

Caco-2, HT29-MTX and RAW264.7 cells were maintained in growth media. The Caco-2 and RAW264.7 cell lines were purchased from the American Type Culture Collection (Manassas, Virginia, USA); HT29-MTX cell line was acquired from Sigma-Aldrich. Caco-2 and HT29-MTX were cultivated in DMEM supplemented with 10% Fetal Bovine Serum (FBS), 100 U mL⁻¹ penicillin and 100 µg mL⁻¹ streptomycin, 1% nonessential amino acids, and 1% GlutaMax supplement (or 2 mM L-alanyl-L-glutamine dipeptide) and incubated at 37 °C in an atmosphere containing 5% CO₂. RAW264.7 cells were cultured in RPMI 1640 medium containing 10% FBS, 100 U mL⁻¹ penicillin/100 µg mL⁻¹ streptomycin, and 1% GlutaMax supplement at 37 °C and 5% CO₂ incubator. Cells were sub-cultivated twice a week for CaCo2/HT29 or 3 times for RAW264.7 cell lines at 70–80% confluence.

Peptide toxicity analysis

Cell viability for Caco2/HT29 in response to the synthetic peptides was evaluated prior to transport assay by using CyQUANT Cell viability in response to peptides in the concentration range: 31.25–2000 µM was measured using 9×10^3 Caco-2 and 1×10^3 HT29-MTX cells per per well (ratio 9:1) grown in a

96-well black plate for 7 days without changing growth media in three replicates. On day 7, growth media was removed and replaced with Hanks' Balanced Salt Solution (HBSS) for 2 h at 37 °C. After removing HBSS, cells were incubated with 100 µL of peptides which were synthesised by Mimotopes Pty. Ltd diluted in HBSS for 2 h. The Caco-2: HT-29 cells were then washed once in HBSS, and cell viability was measured using 100 µL of 0.2% CyQUANT in HBSS. Cells in HBSS were used as control of viable cells. The plates were incubated for 1 h at 37 °C, and fluorescent was measured at 485/530 nm (excitation/emission).

Nitric oxide assay

Nitric oxide (NO) production, measured as nitrite, was determined using diaminonaphthalene (DAN). A cell density of 6×10^4 cells per well sub-cultured RAW264.7 cells (passage number 19) were seeded into 96-well plates in RPMI 1640 phenol red free growth media and incubated for 48 h in 5% CO₂ and a humidified atmosphere at 37 °C. The cultivated cells were exposed to final concentration of 300 ng mL⁻¹ LPS, Quercetin (0.3–100 µM) as positive control and the peptides at concentrations of 2000, 1000, 500, 250, 125, 62.5, and 31.25 µM in three replicates. After 48 h of incubation at 37 °C and 5% CO₂, 20 µL of cell media was transferred into a black 96-well plate. Various concentrations of sodium nitrite standard were added in duplicates to the plate to create a standard curve. A total of 10 µL DAN working reagent (50 µg mL⁻¹) was added into each well followed by 10 min incubation in dark. To stop the reaction, 20 µL of 2.8 N NaOH was added into each well and fluorescence was measured at 360/430 nm (excitation/emission). The nitrite levels in each cell treatment were calculated based on the sodium nitrite standard curve. Cell viability was measure as described in 2–10.

Transepithelial transport of peptides

Caco-2 and HT29-MTX (ratio 9:1) cells were seeded at 4×10^4 cells per well in a growth medium on transwell inserts with polycarbonate membranes (0.4 µm pore size, surface area 0.33 cm²) (Corning, NY, USA). Cells were cultivated for 21 days with growth medium changed twice per week.

After cells were washed with HBSS, monolayer integrity was monitored by transepithelial electrical resistance measurement (TEER) using a Millicell ERS-2 Voltohmmeter (EMD Millipore, Billerica, MA). The growth media was removed and replaced with HBSS for both apical and basolateral chambers for 2 h at 37 °C. HBSS was removed from apical chamber and replaced with peptides (1000 µM in HBSS) and incubated for 2 h at 37 °C. Samples from apical and basolateral chambers were collected and stored at –80 until the further analysis using LC-MS/MS. TEERs were measured at 2, 24, and 48 h post-assay.

LC-MS/MS analysis of transported peptides

Samples from transwells were desalted (Empore SDB-RPS stage tips, Sigma-Aldrich, St Louis, MO, USA). Peptide concentrations were determined by micro-BCA. Peptides (1 µg) were



analysed by LC-MS/MS using a 6500 QTRAP mass spectrometer (SCIEX) coupled to a Shimadzu Nexera UHPLC system employing a C18 column (100 × 2.1 mm, 1.7 μm, 100 Å, Kinetex) at flow rate of 0.4 mL min⁻¹. Solvent A consisted of 0.1% (v/v) formic acid and solvent B was 99.9% (v/v) ACN in 0.1% (v/v) formic acid. A 15 min linear solvent gradient was used with the same buffers described above, starting with 5% to 45% buffer B for 10 min followed 45–80% buffer B for 2 min and then equilibrated with 5% buffer B for 3 min. Declustering potential was 80 eV and a rolling collision energy approach was applied, adjusted according to the precursor ion's mass and charge. An unscheduled MRM mode was used, assigning a 60-second detection window to each transition and a cycle time of 0.6 seconds.

Multiple reaction monitoring (MRM) targeted peptides (e.g., FFGLV, WAMLG, GSGPLP, WTNGPL, LVGAEV, and hydrolysed forms MLG, NGPL). Transitions were analysed in Skyline (version 24.1.0.414), with manual curation.²¹ Quantified peak areas (mean of three replicates) were log₂-transformed prior to statistical analysis (*t*-test, *p* < 0.05).

In silico analysis of peptides

Bioactivity prediction. Potential bioactive peptides in microalgal digesta were identified using a combination of database comparison and computational prediction tools. To initially identify bioactive peptides in the peptide digesta (supernatant and 3–10 kDa fractions), the identified peptides were compared against previously reported bioactive sequences in the BIOPEP-UWM database of bioactive peptides (<https://biochemia.uwm.edu.pl/biopep-uwm/>).²²

To further identify novel potential bioactive peptides, several additional online platforms employing machine learning-based approaches were used. The PeptideRanker tool (https://bioware.ucd.ie/~compass/biowareweb/Server_pages/help/peptideranker/help.php) was applied to prioritise peptides with a high probability of bioactivity, retaining those with scores above 0.8 (where 0.0 indicates a low probability and 1.0 indicates a high probability of bioactivity).²³ Other complementary machine learning-based tools were also used to provide more precise functional annotation and assess different types of therapeutic potential, including CSM-peptides (https://biosig.lab.uq.edu.au/csm_peptides/)²⁴ and PepNet (<https://liulab.top/PepNet/server>).²⁵ Using PepNet, which employs deep learning techniques, anti-inflammatory peptides (AIPs) were further predicted and confirmed.

To improve specificity, dipeptides and tripeptides were excluded, and only peptides with a minimum length of four amino acids were considered for further analysis. The selected peptides were subsequently evaluated for sequence diversity and synthetic feasibility, leading to the identification of five peptides (FFGLV, WAMLG, GSGPLP, WTNGPL, and LPVP) and a negative control (LVGAEV) for experimental validation.

Physicochemical properties. Predicted properties—including isoelectric point, hydrophobicity, charge, and instability index—were calculated for the identified peptides using the Peptides R package.²⁶

Molecular docking analysis. Candidate peptide sequences were subjected to molecular docking to evaluate their potential interactions with the inducible nitric oxide synthase (iNOS) oxygenase domain. The crystal structure of human iNOS (PDB ID: 1NSI, chain A) was retrieved from the Protein Data Bank (PDB) as target for the docking analysis. Peptide structures were modelled using the PEP-FOLD3 web server (<https://bioserv.rpbs.univ-paris-diderot.fr/services/PEP-FOLD3/>) and used as ligands for docking. Each peptide was docked individually against 1NSI. The top-ranked binding poses, based on docking scores, were selected for further analysis. Docked complexes were visualized and analyzed using PyMOL (The PyMOL Molecular Graphics System, Version 3.1, Schrödinger, LLC). Binding sites, interaction types (e.g., hydrogen bonds, hydrophobic interactions), and binding orientation were examined to assess the potential of each peptide as a modulator of iNOS activity. Candidate peptides including FFGLV, WAMLG, GSGPLP, WTNGPL, LVGAEV and LPVP were synthesized to >95% purity by Mimotopes Pty. Ltd (<https://www.mimotopes.com>).

3. Results

Amino acids profiles in peptide digesta

The amino acid profiles of the studied microalgae species are summarized in Table 2. Total amino acid content varied across species, ranging from 19.2 to 43.6 g per 100 g dry weight. *Pandorina* sp. exhibited the highest amino acid content (43.6% total amino acids and 17.6% EAA), followed by *Glaucocystis nostochinearum* (35.0% total amino acids and 12.7% EAA). Lysine one of the essential amino acids was the most abundant (1.7–4.4 g per 100 g), followed by leucine (1.1–2.4 g per 100 g) and threonine (1.3–2.5 g per 100 g).

Characterisation of peptide digesta

Peptidomic profiling was performed on three peptide fractions generated by *in vitro* gastrointestinal digestion (INFOGEST) of eight different microalgae species: the supernatant and two size-fractionated pellet fractions. Fig. 1 summarises the number of peptides identified *via de novo* sequencing in at least two out of three biological replicates across all fractions for each species.

The supernatant fraction contained relatively few unique peptides across the eight microalgae species studied. The highest peptide count was observed in *Rhodomonas salina* (27 peptides), followed by *Pandorina* sp. (19 peptides, Fig. 1a). Peptide masses in the supernatant primarily ranged between 246.1 and 649.3 (*m/z*) (SI Table S1) and were predominantly singly charged (Fig. 1c). Peptide lengths spanned 2 to 7 amino acids; notably, only one peptide with 7 amino acids was identified in *Arthrospira platensis* (Fig. 1b).

As anticipated, a larger diversity and number of peptides were detected in the pellet fractions. Generally, the 3–10 kDa fraction contained more unique peptides than the >10 kDa fraction for most species. However, *Arthrospira platensis* and *Desmodesmus arthrodesmiformis* showed the reverse pattern,



Table 2 Amino acid profiles of the studied microalgae species

Row	ANACC identifier	Microalgae species	EAA													Non-EAA													Total
			His	Ile	Leu	Lys	Met	Phe	Thr	Val	Ala	Arg	Asx	Glx	Gly	Pro	Ser	Tyr	Total EAA										
1	CS946	<i>Pandorina</i> sp.	2.2	1.2	2.4	4.4	0.6	2.7	2.5	1.6	2.7	6.6	4.7	4.6	2.2	1.5	2.3	1.4	17.6	43.6									
2	CS777	<i>Glaucocystis nostochinearum</i>	1.7	0.8	1.8	3.3	0.4	1.7	1.9	1.2	2.7	6.7	3.6	3.8	1.8	1.3	1.6	1.0	12.7	35.0									
3	CS950	<i>Desmodium arthrodesmiformis</i>	1.7	1.0	1.8	3.2	0.5	1.9	2.0	1.4	2.3	3.9	3.6	3.8	1.9	1.2	1.9	1.4	13.5	33.4									
4	CS416	<i>Nannochloropsis australis</i>	1.4	0.8	1.7	2.7	0.5	1.7	1.9	1.1	1.9	3.1	3.0	3.7	1.6	2.1	1.7	1.2	11.8	30.1									
5	CS174	<i>Rhodomonas salina</i>	1.2	0.7	1.3	2.3	0.6	1.5	1.6	1.0	1.7	2.7	2.7	2.8	1.3	0.8	1.5	1.7	10.2	25.4									
6	CS697	<i>Arthrospira platensis</i>	1.1	0.9	1.3	1.9	0.4	1.3	1.5	1.1	1.5	2.6	2.5	3.0	1.2	0.7	1.5	1.2	9.5	23.7									
7	CS977	<i>Chlamydomonas</i> sp.	1.2	0.8	1.3	2.0	0.5	1.4	1.5	1.0	1.6	2.5	2.3	2.5	1.2	1.0	1.4	1.3	9.6	23.5									
8	CS1224	<i>Snowella</i> sp.	1.0	0.7	1.1	1.7	0.4	1.1	1.3	0.8	1.3	2.0	1.9	2.2	1.0	0.7	1.3	0.6	8.0	19.2									

Values are presented in g per 100 g dried material. The results for Asp and Glu include contribution of Asn and Glm respectively, as they converted during hydrolysis. Glx represents both Glu and Glu and Asx represents Asp as well as Asn. Trp and Cys were not measured in this study.

with more peptides detected in the >10 kDa fraction (Fig. 1a). Peptide mass distributions ranged from 350.6–1206.1 Da in the 3–10 kDa fraction and from 404.2–2837.3 in the >10 kDa fraction (SI Table S1). Most peptides in the >10 kDa fraction (93.1%) carried a +2 charge, while the 3–10 kDa fraction contained primarily singly charged peptides, with only 24.5% doubly charged (SI Table S1 and Fig. 1d).

Peptide sequence lengths in the 3–10 kDa fraction ranged from 4 to 23 amino acids, with a modal length of 5 amino acids. In the >10 kDa fraction, sequences spanned 4 to 26 amino acids, with a predominant length of 8 amino acids (Fig. 1c).

A total of six peptides (17%) were common to both the supernatant and the 3–10 kDa fraction, but none were found in both the supernatant and >10 kDa fraction. Additionally, 95 peptides were shared between the 3–10 kDa (8.3% of total) and >10 kDa (14%; Fig. 1b). Peptides and proteins in >10 kDa fraction were further identified *via* database search against a custom in-house microalgae protein database.

Physicochemical properties of peptides

The physicochemical characteristics of peptides—including isoelectric point, instability index, hydrophobicity—were analysed across the three fractions. Significant differences in hydrophobicity were observed among the three fractions. Peptides in the supernatant exhibited the highest hydrophobicity, which was significantly greater than in both pellet fractions (>10 kDa *vs.* supernatant and 3–10 kDa: $p < 10^{-5}$; supernatant *vs.* 3–10 kDa: $p < 0.05$; Fig. 1e).

The instability index, which reflects the predicted peptide stability, also differed significantly between the three fractions ($p < 0.05$). Only one-third of the peptides in the supernatant fraction exhibited an instability index below 40, the threshold for stability,²⁷ compared to 78% in the 3–10 kDa fraction and 76% in the >10 kDa fraction. This indicates that most peptides in the supernatant are less stable than those in the pellet fractions.

Most peptides in the supernatant fraction (62%) had an isoelectric point of 6.1, while a broader distribution of isoelectric points was seen in both pellet fractions (Fig. 1e). These analyses guided the selection of candidate peptides for further investigation of bioactivity and bioavailability.

Algal bioactive peptides

Potential bioactive peptides in microalgal digesta were identified using two approaches: (1) comparison with previously reported bioactive peptides; and (2) prediction using machine learning based tools such as PeptideRanker, CSM-peptides, and PepNet.^{23–25} Dipeptides and tripeptides were excluded from this analysis, as these are commonly produced from a broad array of dietary proteins and are less likely to be unique to microalgae. Only peptides of at least four amino acids in length were analysed.

Among all identified peptides, only three with previously documented bioactivity were identified from the digesta of supernatant and 3–10 kDa. Due to the use of *de novo* sequen-



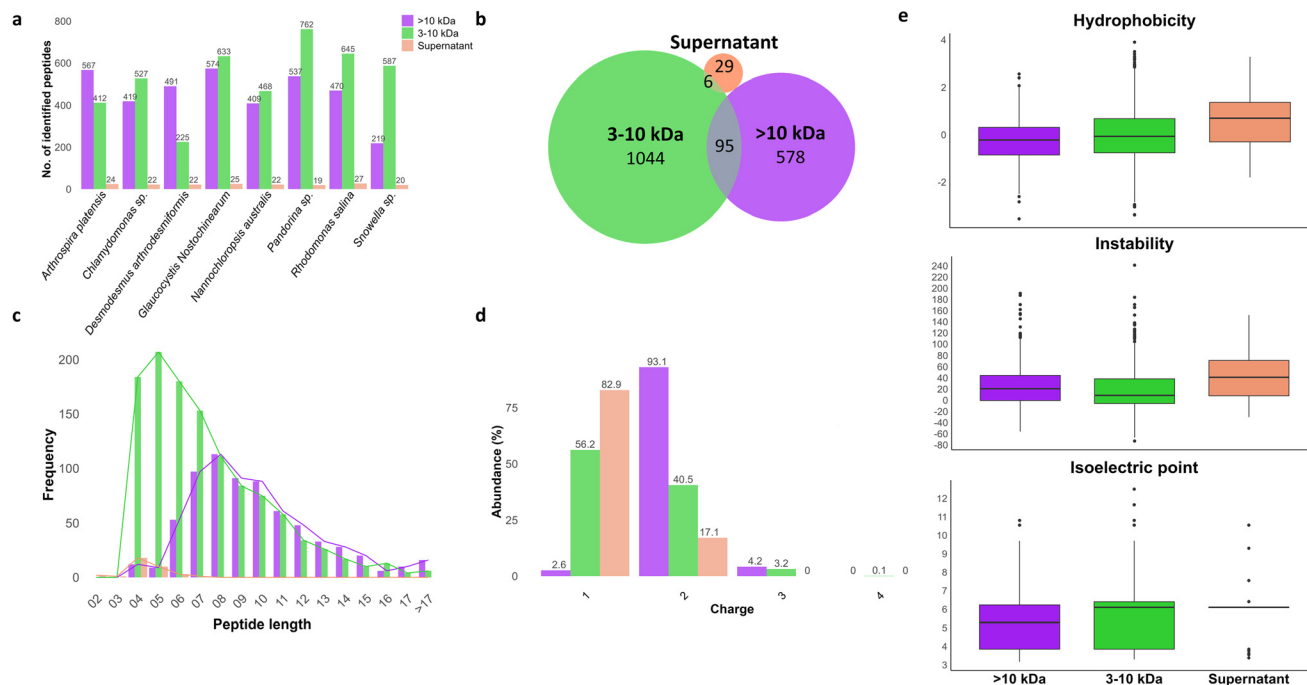


Fig. 1 Peptide profiling in supernatant and size-fractionated pellet fractions. a. Number of peptides identified by *de novo* sequencing across eight microalgae species. b. Overlap of reproducibly identified peptides (Venn diagram). c. Distribution of peptide sequence lengths. d. Charge state distribution of peptides (+1 to +4). e. Comparison of physicochemical properties of proteins (hydrophobicity, instability, and isoelectric point) of peptides, visualised as box plots.

cing, leucine (L) in these sequences may represent leucine or its isomer, isoleucine (I).²⁸ The peptide LPVP (a known dipeptidyl peptidase IV inhibitor, DPP IV inhibitor) was present in the supernatant of all eight microalgal species. In the 3–10 kDa fraction, LPPV (a PEP inhibitor) and LLAP (another DPP IV inhibitor) were found (BIOPEP-UWM database). LPPV was present in all species other than *Arthrospira platensis*, while LLAP was present in five of the species: *Arthrospira platensis*, *Chlamydomonas* sp., *Glaucozystis Nostochinearum*, *Pandorina* sp. and *Rhodomonas salina*. Overall, these findings indicate that bioactive peptides were broadly conserved across species, with minor differences in their distribution.

Following the identification of potential bioactive peptides, a stepwise filtering pipeline was employed to prioritise peptide candidates for synthesis. Initial screening retained peptides with a PeptideRanker bioactivity scores above 80%. The refined set was further evaluated based on physicochemical parameters, with emphasis on stability and functionality under small intestinal conditions. Those peptides were retained with high stability (instability index < 40), moderate hydrophobicity, and an isoelectric point between 6.0 and 6.4, approximating the pH range of the small intestine.²⁹ Finally, peptides were manually assessed for sequence diversity and synthetic feasibility, resulting in the selection of five peptides along with a negative control for experimental validation. Of eight peptides meeting these criteria, four (FFGLV, WAMLG, GSGPLP, and WTNGPL) as well as LPVP and LVGAEV were synthesised for experimental validation. Notably, all the bioactive

peptide candidates were present in the 3–10 kDa fraction in *Snowella* sp. Interestingly, LVGAEV was predicted to have a low probability of bioactivity by PeptideRanker (5%) and was not classified as anti-inflammatory by CSM-peptides or PepNet yet showed binding affinity to the active site of human inducible nitric oxide synthase (1NSI) in molecular docking studies.

The interactions between Val6 of the LVGAEV peptide with Ala282 and Arg266, both of which are located near the substrate access channel, suggesting potential influence on enzymatic activity. Moreover, the interaction between Ala4 with H4B600, a residue adjacent to the cofactor binding site, potentially contributes to conformational stabilization (SI Fig. S1). Hydrogen bonding was also observed between Glu5 with Thr121 and Tyr492, residues located near the heme group. Two hydrogen bonds of Gly3 with Arg3888, with interaction distances of 3.2 Å and 2.6 Å, reinforcing the binding of the peptide within the active pocket. Interestingly, the only peptide that showed anti-inflammatory properties was LVGAEV based on *in vitro* cell assay (Fig. 2a).

Transepithelial transport of peptides in a Caco-2/HT-29 transwell model

The transport of five synthesised peptides across an intestinal epithelial barrier was assessed using a co-culture transwell model with Caco-2 and HT-29 cells. Peptide translocation from the apical (AP) to the basolateral (BL) compartment was monitored by a multiple reaction monitoring mass spectrometry



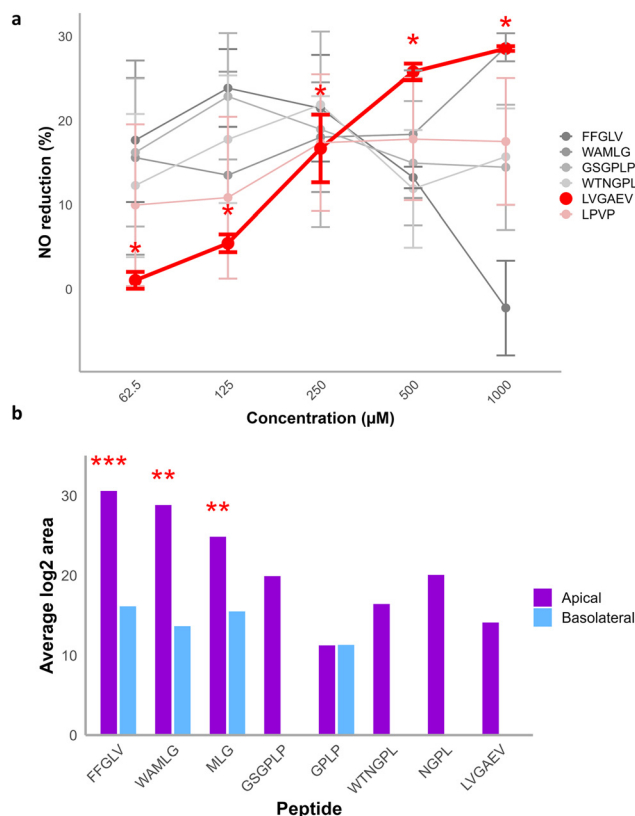


Fig. 2 Peptides bioactivity and transport across Caco-2 monolayers. a. NO inhibitory activity of six peptides at varying concentrations, measured in LPS-induced RAW264.7 cells. Data are presented as mean \pm SD ($n = 3$). The peptide LVGAEV is highlighted in bold to indicate statistically significant reduction in NO production ($p < 0.05$) compared to LPS, as shown by the asterisk. b. Bioavailability of peptides and their hydrolysed forms (MLG, GPLP, and NGPL) assessed using a Caco-2 transwell model. The average log₂-transformed area (intensity) of each peptide in the apical and basolateral compartments was quantified by MRM. Bars represent mean intensities, with asterisks showing significant differences between compartments ($p < 0.05$). Missing bars indicate undetected peptides in the respective compartment.

(MRM-MS)-based quantitation method. In addition to the intact peptides, hydrolysed forms of WAMLG and GSGPLP, generated by brush border peptidases (e.g., dipeptidyl peptidase IV), were also tracked. Basolateral transport was observed for FFGLV and WAMLG, along with MLG, the hydrolysed product of WAMLG. For all three peptides, the ion intensities were significantly lower in the BL compartment compared to the AP side, indicating partial permeability across the epithelial monolayer. Although intact GSGPLP was not identified in the BL compartment, its degradation product, GPLP, was identified in both AP and BL compartments, with comparable log₂ ion intensities (11.27 and 11.32, respectively) (Fig. 2b). This suggests successful translocation of the degraded peptide across the monolayer. In contrast, WTNGPL, its hydrolysis product NGPL, and LVGAEV were not identified in the BL compartment, indicating limited or absent permeability under the experimental conditions.

Digestion-resistant peptides

To characterize microalgal peptides resistant to gastrointestinal digestion, peptides larger than 10 kDa present in the pellet (undigested fraction) were subjected to FASP in-solution digestion method and the tryptic peptides were identified using both *de novo* and database search. Out of 17 identified proteins in the undigested fraction (>10 kDa fraction), 7 were photosynthetic proteins with the Gene Ontology (GO) term GO:0015979. These included well-known structural and functional proteins such as ribulose biphosphate carboxylase large chain, chlorophyll a-b binding protein, photosystem II CP47 reaction center protein. Photosynthetic proteins were detected as digestion-resistant components in at least one species among all microalgae studied, except for *Arthrospira platensis*, *Desmodesmus arthrodesmiformis*, and *Pandorina* sp., where such proteins were absent in the undigested fraction (Fig. 3). In *Glaucozystis Nostochinearum*, three of the four proteins present in the >10 kDa fraction also belonged to the photosynthesis gene ontology group (Fig. 3). This highlights the notable resistance of certain photosynthetic proteins to enzymatic digestion, consistent with their robust structural roles in algal cells. Additionally, several uncharacterised pro-

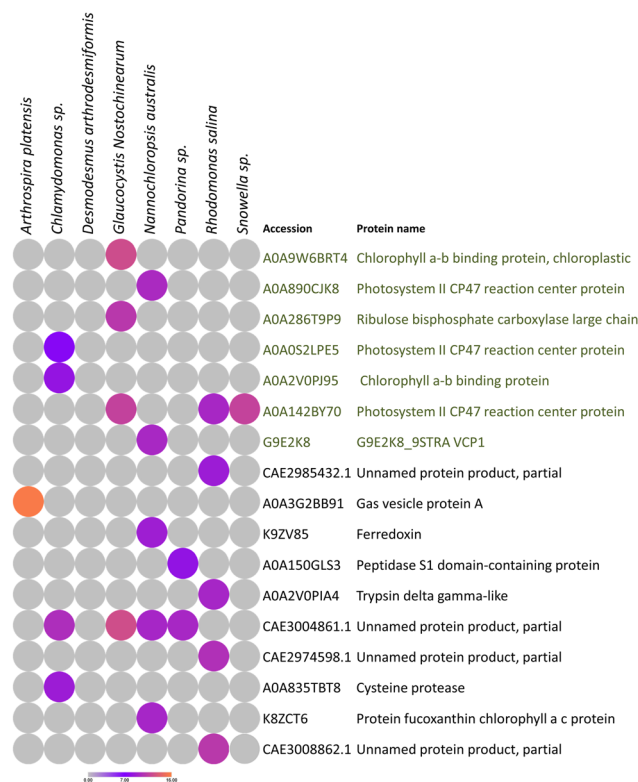


Fig. 3 Peptide profiling in supernatant and size-fractionated pellet fractions. a. Number of peptides identified by *de novo* sequencing across eight microalgae species. b. Overlap of reproducibly identified peptides (Venn diagram). c. Distribution of peptide sequence lengths. d. Charge state distribution of peptides (+1 to +4). e. Comparison of physicochemical properties of proteins (hydrophobicity, instability, and isoelectric point) of peptides, visualised as box plots.



teins were identified as digestion resistant. Notably, the protein CAE3004861.1 from *Rhodomonas lens* was present in four different microalgal species, suggesting a conserved resistance pattern among some unannotated proteins in the microalgal lineage.

The potential allergenicity of proteins in the undigested fraction was assessed using AlgPred 2.0, a comprehensive web-based tool that integrates machine learning with motif, BLAST, and IgE epitope mapping approaches for allergen prediction.³⁰ Two allergenic peptide motifs—NNACEAFLCNCNDR and DNVEGFNCER—were detected, with machine learning (ML) scores of 0.4 and 0.35, respectively. The motif-emerging and with classes-identification (MERICI) score for both motifs were 0.5, indicating their presence matches experimentally validated IgE epitopes. These findings suggest that digestion-resistant proteins in microalgae may possess peptide sequences with allergenic potential, warranting further validation in allergenicity risk assessments.

4. Discussion

The nutritional value of microalgae as a novel food is closely tied to their protein quality, which is determined by essential amino acid composition and ileal protein digestibility. The EAA content in *Pandorina* sp. (17.6%) is comparable to high-quality animal-based proteins, such as egg with 16.5% EAA (Gorissen *et al.*, 2018).³¹ All eight microalgal species evaluated showed high lysine content, an amino acid often deficient in cereal grains such as wheat, corn and rice; as well as in legumes like fava bean.³²

Downstream processing techniques prior to digestibility analysis or use of crude protein rather than whole biomass, have been shown to significantly enhance protein digestibility.^{33,34} Pre-treatment methods, such as cell wall disruption by ball-milling, were employed in this study to maximise protein accessibility in whole algal biomass prior to *in vitro* digestion, an approach that aimed to reflect consumption of whole biomass *in vivo*.

In protein digestibility studies, 80% (v/v) methanol precipitation is commonly used to distinguish undigested proteins and high molecular weight peptides (pellet) from low molecular weight peptides and free amino acids (supernatant) (Santos-Hernández *et al.*, 2018; Sousa *et al.*, 2023).^{7,35} However, our findings reveal that methanol precipitation is not fully effective to separate digested from undigested fractions. Size fractionation demonstrated that digested peptides remained in the pellet, likely as a result of their hydrophobicity or low solubility which causes them to aggregate and precipitate.³⁶ This indicates that using 80% (v/v) methanol precipitation may underestimate the pool of potentially digestible and permeable peptides. Sampling at the end of the *in vitro* digestibility assay (intestinal phase) allowed us to capture peptides after multiple and combined enzymatic degradation, thus explaining the predominance of smaller peptides (mostly di- to pentapeptide) and free amino acids.³⁷ To enhance detection, we

optimised liquid chromatography-mass spectrometry (LC-MS) method with a pentafluorophenyl (PFP) column for better retention and separation of short peptides, instead of the C18 column which is commonly used in proteomics studies. *De novo* interpretation of MS/MS spectra was used to identify the peptides as most were too short for confident identification through database searching and spectral matching algorithms.³⁷

Characterisation of the undigested fraction (>10 kDa) revealed a set of proteins and peptides that were resistant to digestion. Several proteins identified in the >10 kDa pellet fraction were associated with photosynthetic processes (GO:0015979), indicating that structural or membrane-associated proteins involved in photosynthesis may be more resistant to enzymatic digestion. The identification of proteins such as ribulose biphosphate carboxylase and chlorophyll a-b binding protein across multiple species suggests a conserved resistance among photosynthetic machinery to gastrointestinal digestion. Resistance of photosynthetic protein complexes such as chlorophyll a-b binding proteins, and photosystem I (PSI) and II (PSII) in spinach (*Spinacia oleracea*) leaves to digestive enzymes even after extended exposure to pancreatic juice has been demonstrated previously.³⁸

Interestingly, literature suggests that delayed gastrointestinal digestion of thylakoid-rich plants—such as those containing photosynthetic protein complexes—can promote satiety and contribute to appetite regulation, potentially aiding in obesity prevention.^{35,38,39} While plant thylakoids contain lipids, pigments, and proteins, the resistance of specific proteins (*e.g.*, chlorophyll a-b binding protein, PSI, PSII) to digestion may contribute to satiety, suggesting that similar proteins in microalgae may act in a similar way.

On the other hand, proteins or peptides that resist gastrointestinal digestion are more likely to reach the gut immune system intact and potentially elicit allergic responses.⁴⁰ Our *in silico* analysis of peptides from >10 kDa fraction identified two putative allergenic motifs of NNACEAFLCNCNDR and DNVEGFNCER in the undigested fraction. While these motifs overlapped with experimentally validated IgE epitopes, suggesting potential allergenicity, this will require immunological and clinical validation. For bioactive peptide screening, this study integrated several approaches: physicochemical property analysis, *in silico* bioactivity prediction, molecular docking, and experimental validation.^{41,42} Initial filtering of excluded peptide sequences predicted to be unstable or poorly soluble under physiological conditions, focusing on those with greater functional potential. Our findings revealed that machine learning-based prediction tools alone are insufficient to reliably identify putative bioactive peptides. The results obtained from different prediction tools may vary; for example, the peptide EALPE which was assigned a low bioactivity probability (0.1%) by PeptideRanker—a widely used software tool⁴¹—was predicted by PepNet to be a putative antimicrobial with a probability of 94.4%. This inconsistency highlights a major limitation of relying on a single predictive model and underscores the importance of using multiple, complementary algorithms when screening for functional peptides.



The limitations of *in silico* prediction were further illustrated by LVGAEV, a peptide that was not predicted as bioactive peptide based on PeptideRanker but demonstrated significant *in vitro* anti-inflammatory activity, as shown by the reduction of nitric oxide (NO) production in LPS-stimulated RAW264.7 cells. Using molecular docking showed LVGAEV interacts with the oxygenase domain of human iNOS, suggesting this peptide's anti-inflammatory effect is mechanistically plausible. This example demonstrates how structure-based computational tools can complement machine learning by elucidating target interactions that explain observed bioactivity.

In contrast, peptides predicted to be anti-inflammatory (FFGLV and WAMLG) did not reduce NO production in the *in vitro* model. These discrepancies highlight the gap between computational predictions and actual biological activity, reinforcing the necessity of experimental confirmation.

The results from the transwell permeability assays further illustrate the complexities of peptide bioactivity. Peptide hydrolysis, poor solubility, or aggregation within the cell culture medium could diminish the effective concentration at intracellular targets, limiting measurable bioactivity despite favourable *in silico* scores.⁴³ Therefore, the functional impact of food-derived peptides depends not only on their predicted properties and target interactions but also on their bioavailability and stability in biological contexts. This may highlight the importance of animal digestive models to more effectively evaluate the bioavailability, functionality and safety of potential bioactive peptides from novel foods such as microalgae.

Our findings on algal bioactive peptides demonstrate that a multi-pronged screening pipeline—incorporating physicochemical profiling, using diverse computational tools, structure-based docking, and experimental validation—enables a more robust characterisation and selection of peptides with nutritional and therapeutic potential.

5. Conclusion

With a growing need for high quality dietary protein for the global population, here we show supporting evidence for eight microalgae species that are not commonly consumed. All studied species had high lysine content, reinforcing their value in complementing lysine-deficient plant-based diets.³²

To our knowledge, this is the first study to analyse both digested and undigested peptide fractions in microalgae enabling the identification of digestion-resistant peptides that might otherwise be overlooked. By examining the pellet fraction—typically considered the undigested fraction following *in vitro* digestion using INFOGEST protocols—we uncovered additional permeable and bioactive peptides, broadening the nutritional and functional landscape of microalgae-derived proteins. This work also represents the first in-depth peptide mapping across multiple microalgae species.

Our findings highlight the complexity of food-derived peptide bioactivity and support the need for a comprehensive strategy that combines multiple predictive models (rather than relying on

one model), physicochemical screening, structural modelling, and *in vitro* biological validation to more reliably identify and characterise functional peptides. Notably, discrepancies between *in silico* predictions and *in vitro* outcomes—such as the lack of anti-inflammatory activity of predicted peptides FFGLV and WAMLG—demonstrate that computational approaches alone are insufficient and must be complemented by experimental validation. Future research should focus on *in vivo* validation of identified peptides and their physiological effects to further identify the potential of microalgae as a sustainable, functional food to support health, wellbeing and disease prevention.

Author contributions

Sara Hamzelou: conceptualization, methodology, formal analysis, investigation, data curation, software, visualization, writing – original draft. Damien Belobrajdic: supervising, conceptualization, writing – review & editing. Henri Brook: methodology, writing – review & editing. Wei Chen: methodology. Fletcher Hiten: methodology. Kim Lee Chang: methodology. Diane Purcell: methodology. Utpal Bose: methodology, writing – review & editing. Simone Osborne: methodology. Cassandra Pegg: methodology, writing – review & editing. Michelle L. Colgrave: supervising, conceptualization, writing – review & editing.

Conflicts of interest

The authors declare that they have no known competing financial interests or personal relationships that could have appeared to influence the work reported in this paper.

Abbreviations

AAA	Aromatic amino acids
ANACC	Australian National Algae Culture Collection
COST	Cooperation in Science and Technology
EAA	Essential amino acids
FASP	Filter-aided sample preparation
FDR	False discovery rate
GO	Gene ontology
HBSS	Hanks' balanced salt solution
iNOS	Inducible nitric oxide synthase
LC-MS	Liquid chromatography-mass spectrometry
MRM	Multiple reaction monitoring
NO	Nitric oxide
PSMs	Peptide-spectrum matches
SAA	Sulfur amino acid
TEER	Transepithelial electrical resistance measurement

Data availability

All data supporting this study, including detailed peptide sequences and mass spectrometry parameters, are provided



within the article and its supplementary information (SI).
Supplementary information: supplementary data 1 and data 2.
See DOI: <https://doi.org/10.1039/d6fo00231e>.

Acknowledgements

S. H. would like to acknowledge scholarship support from the Commonwealth Scientific and Industrial Research Organisation (CSIRO) Early Research Career (CERC) postdoctoral fellowship. M. C. is supported by the Australian Research Council Centre of Excellence for Innovations in Peptide and Protein Science (CE200100012).

References

- 1 S. Hamzelou, D. Belobrajdic, J. A. Broadbent, A. Juhász, K. Lee Chang, I. Jameson, *et al.*, Utilizing proteomics to identify and optimize microalgae strains for high-quality dietary protein: a review, *Crit. Rev. Biotechnol.*, 2024, **44**(7), 1280–1295.
- 2 Y. Torres-Tiji, F. J. Fields and S. P. Mayfield, Microalgae as a future food source, *Biotechnol. Adv.*, 2020, **41**, 107536.
- 3 M. P. Caporgno and A. Mathys, Trends in Microalgae Incorporation Into Innovative Food Products With Potential Health Benefits, *Front. Nutr.*, 2018, **5**, 58.
- 4 T. S. Bingeman, D. H. Perlman, D. G. Storey and I. A. Lewis, Digestomics: an emerging strategy for comprehensive analysis of protein catabolism, *Curr. Opin. Biotechnol.*, 2017, **43**, 134–140.
- 5 J. Renukuntla, A. D. Vadlapudi, A. Patel, S. H. Boddu and A. K. Mitra, Approaches for enhancing oral bioavailability of peptides and proteins, *Int. J. Pharm.*, 2013, **447**(1–2), 75–93.
- 6 M. Minekus, M. Alminger, P. Alvito, S. Ballance, T. Bohn, C. Bourlieu, *et al.*, A standardised static in vitro digestion method suitable for food – an international consensus, *Food Funct.*, 2014, **5**(6), 1113–1124.
- 7 R. Sousa, I. Recio, D. Heimo, S. Dubois, P. J. Moughan, S. M. Hodgkinson, *et al.*, In vitro digestibility of dietary proteins and in vitro DIAAS analytical workflow based on the INFOGEST static protocol and its validation with in vivo data, *Food Chem.*, 2023, **404**, 134720.
- 8 Dietary protein quality evaluation in human nutrition. Report of an FAQ Expert Consultation, *FAO Food Nutr. Pap.*, 2013, **92**, 1–66.
- 9 A. Brodkorb, L. Egger, M. Alminger, P. Alvito, R. Assunção, S. Ballance, *et al.*, INFOGEST static in vitro simulation of gastrointestinal food digestion, *Nat. Protoc.*, 2019, **14**(4), 991–1014.
- 10 Z. Karami and B. Akbari-Adergani, Bioactive food derived peptides: a review on correlation between structure of bioactive peptides and their functional properties, *J. Food Sci. Technol.*, 2019, **56**(2), 535–547.
- 11 T. Wijesekara, E. Abeyrathne and D. U. Ahn, Effect of Bioactive Peptides on Gut Microbiota and Their Relations to Human Health, *Foods*, 2024, **13**(12), 1853.
- 12 J. D. Cruz and V. Vasconcelos, Legal Aspects of Microalgae in the European Food Sector, *Foods*, 2024, **13**(1), 124.
- 13 S. Thangsiri, W. Inthachat, P. Temviriyankul, Y. Sahasakul, P. Trisonthi, W. Pan-utai, *et al.*, Bioactive compounds and in vitro biological properties of *Arthrospira platensis* and *Athrospira maxima*: a comparative study, *Sci. Rep.*, 2024, **14**(1), 23786.
- 14 S. Hamzelou, D. Belobrajdic, A. Juhász, H. Brook, U. Bose, M. L. Colgrave, *et al.*, Nutrition, allergenicity and physicochemical qualities of food-grade protein extracts from *Nannochloropsis oculata*, *Food Chem.*, 2023, **424**, 136459.
- 15 C. Latsos, E. Wassenaar, T. Moerdijk, B. Coleman, J. Robbens, S. van Roy, *et al.*, Effect of pH on *Rhodomonas salina* growth, biochemical composition, and taste, produced in semi-large scale under sunlight conditions, *J. Appl. Phycol.*, 2022, **34**(3), 1215–1226.
- 16 C. J. S. Bolch and S. I. Blackburn, Isolation and purification of Australian isolates of the toxic cyanobacterium *Microcystis aeruginosa* Kütz., *J. Appl. Phycol.*, 1996, **8**(1), 5–13.
- 17 R. R. L. Guillard and J. H. Ryther, Studies of marine planktonic diatoms: I. *Cyclotella nana* Hustedt, and *Detonula confervacea* (Cleve) Gran, *Can. J. Microbiol.*, 1962, **8**(2), 229–239.
- 18 A. R. Loeblich III, A Seawater Medium for Dinoflagellates and the Nutrition of *Cachonina NIEI*, *J. Phycol.*, 1975, **11**(1), 80–86.
- 19 S. O. Lourenço, E. Barbarino, P. L. Lavín, U. M. L. Marquez and E. Aïdar, Distribution of intracellular nitrogen in marine microalgae: Calculation of new nitrogen-to-protein conversion factors, *Eur. J. Phycol.*, 2004, **39**(1), 17–32.
- 20 M. Minekus, M. Alminger, P. Alvito, S. Ballance, T. Bohn, C. Bourlieu, *et al.*, A standardised static in vitro digestion method suitable for food – an international consensus, *Food Funct.*, 2014, **5**(6), 1113–1124.
- 21 B. MacLean, D. M. Tomazela, N. Shulman, M. Chambers, G. L. Finney, B. Frewen, *et al.*, Skyline: an open source document editor for creating and analyzing targeted proteomics experiments, *Bioinformatics*, 2010, **26**(7), 966–968.
- 22 P. Minkiewicz, A. Iwaniak and M. Darewicz, BIOPEP-UWM Database of Bioactive Peptides: Current Opportunities, *Int. J. Mol. Sci.*, 2019, **20**(23), 5978.
- 23 C. Mooney, N. J. Haslam, G. Pollastri and D. C. Shields, Towards the improved discovery and design of functional peptides: common features of diverse classes permit generalized prediction of bioactivity, *PLoS One*, 2012, **7**(10), e45012.
- 24 C. H. M. Rodrigues, A. Garg, D. Keizer, D. E. V. Pires and D. B. Ascher, CSM-peptides: A computational approach to rapid identification of therapeutic peptides, *Protein Sci.*, 2022, **31**(10), e4442.
- 25 J. Han, T. Kong and J. Liu, PepNet: an interpretable neural network for anti-inflammatory and antimicrobial peptides



- prediction using a pre-trained protein language model, *Commun. Biol.*, 2024, **7**(1), 1198.
- 26 D. Osorio, P. Rondón-Villarreal and R. Torres, Peptides: A package for data mining of antimicrobial peptides, *R J.*, 2015, **7**(1), 4–14.
- 27 K. Guruprasad, B. V. B. Reddy and M. W. Pandit, Correlation between stability of a protein and its dipeptide composition: A novel approach for predicting in vivo stability of a protein from its primary sequence, *Protein Eng., Des. Sel.*, 1990, **4**(2), 155–161.
- 28 R. S. Johnson, B. C. Searle, B. L. Nunn, J. M. Gilmore, M. Phillips, C. T. Amemiya, *et al.*, Assessing Protein Sequence Database Suitability Using De Novo Sequencing, *Mol. Cell. Proteomics*, 2020, **19**(1), 198–208.
- 29 V. V. Khutoryanskiy, Longer and safer gastric residence, *Nat. Mater.*, 2015, **14**(10), 963–964.
- 30 N. Sharma, S. Patiyal, A. Dhall, A. Pande, C. Arora and G. P. S. Raghava, AlgPred 2.0: an improved method for predicting allergenic proteins and mapping of IgE epitopes, *Brief. Bioinform.*, 2021, **22**(4), bbaa294.
- 31 S. H. M. Gorissen and O. C. Witard, Characterising the muscle anabolic potential of dairy, meat and plant-based protein sources in older adults, *Proc Nutr Soc.*, 2018, **77**(1), 20–31.
- 32 L. Herreman, P. Nommensen, B. Pennings and M. C. Laus, Comprehensive overview of the quality of plant- And animal-sourced proteins based on the digestible indispensable amino acid score, *Food Sci. Nutr.*, 2020, **8**(10), 5379–5391.
- 33 S. S. Ali, R. Al-Tohamy, M. Al-Zahrani, M. Schagerl, M. Kornaros and J. Sun, Advancements and challenges in microalgal protein production: A sustainable alternative to conventional protein sources, *Microb. Cell Fact.*, 2025, **24**(1), 61.
- 34 L. Machado, G. Carvalho and R. N. Pereira, Effects of Innovative Processing Methods on Microalgae Cell Wall: Prospects towards Digestibility of Protein-Rich Biomass, *Biomass*, 2022, **2**(2), 80–102.
- 35 M. Santos-Hernández, B. Miralles, L. Amigo and I. Recio, Intestinal Signaling of Proteins and Digestion-Derived Products Relevant to Satiety, *J. Agric. Food Chem.*, 2018, **66**(39), 10123–10131.
- 36 L. Malavolta, M. R. Pinto, J. H. Cuvero and C. R. Nakaie, Interpretation of the dissolution of insoluble peptide sequences based on the acid-base properties of the solvent, *Protein Sci.*, 2006, **15**(6), 1476–1488.
- 37 R. Portmann, P. Jiménez-Barrios, J. Jardin, L. Abbühl, D. Barile, M. Danielsen, *et al.*, A multi-centre peptidomics investigation of food digesta: current state of the art in mass spectrometry analysis and data visualisation, *Food Res. Int.*, 2023, **169**, 112887.
- 38 S. C. Emek, H. E. Åkerlund, M. Clausén, L. Ohlsson, B. Weström, C. Erlanson-Albertsson, *et al.*, Pigments protect the light harvesting proteins of chloroplast thylakoid membranes against digestion by gastrointestinal proteases, *Food Hydrocoll.*, 2011, **25**(6), 1618–1626.
- 39 E.-L. Stenblom, B. Weström, C. Linninge, P. Bonn, M. Farrell, J. F. Rehfeld, *et al.*, Dietary green-plant thylakoids decrease gastric emptying and gut transit, promote changes in the gut microbial flora, but does not cause steatorrhea, *Nutr. Metab.*, 2016, **13**(1), 67.
- 40 K. L. Bøgh and C. B. Madsen, Food Allergens: Is There a Correlation between Stability to Digestion and Allergenicity?, *Crit. Rev. Food Sci. Nutr.*, 2016, **56**(9), 1545–1567.
- 41 A. Vidal-Limon, J. E. Aguilar-Toalá and A. M. Liceaga, Integration of Molecular Docking Analysis and Molecular Dynamics Simulations for Studying Food Proteins and Bioactive Peptides, *J. Agric. Food Chem.*, 2022, **70**(4), 934–943.
- 42 Z. Du, J. Comer and Y. Li, Bioinformatics approaches to discovering food-derived bioactive peptides: Reviews and perspectives, *TrAC, Trends Anal. Chem.*, 2023, **162**, 117051.
- 43 C. F. Le, C. M. Fang and S. D. Sekaran, Intracellular Targeting Mechanisms by Antimicrobial Peptides, *Antimicrob. Agents Chemother.*, 2017, **61**(4), e02340–16.

